A novel radioprotective function for the mitochondrial tumor suppressor protein Fus1

EM Yazlovitskaya[1,2], R Uzhachenko[3], PA Voziyan[1], WG Yarbrough[4,5,6] and AV Ivanova*[4]

FUS1/TUSC2 is a mitochondrial tumor suppressor with activity to regulate cellular oxidative stress by maintaining balanced ROS production and mitochondrial homeostasis. Fus1 expression is inhibited by ROS, suggesting that individuals with a high level of ROS may have lower Fus1 in normal tissues and, thus, may be more prone to oxidative stress-induced side effects of cancer treatment, including radiotherapy. As the role of Fus1 in the modulation of cellular radiosensitivity is unknown, we set out to determine molecular mechanisms of Fus1 involvement in the IR response in normal tissues. Mouse whole-body irradiation methodology was employed to determine the role for Fus1 in the radiation response and explore underlying molecular mechanisms. Fus1$^{-/-}$ mice were more susceptible to radiation compared with Fus1$^{+/+}$ mice, exhibiting increased mortality and accelerated apoptosis of the GI crypt epithelial cells. Following untimely reentrance into the cell cycle, the Fus1$^{-/-}$ GI crypt cells died at accelerated rate via mitotic catastrophe that resulted in diminished and/or delayed crypt regeneration after irradiation. At the molecular level, dysregulated dynamics of activation of main IR response proteins (p53, NFκB, and GSK-3β), as well as key signaling pathways involved in oxidative stress response (SOD2, PRDX1, and cytochrome *c*), apoptosis (BAX and PARP1), cell cycle (Cyclins B1 and D1), and DNA repair (γH2AX) were found in Fus1$^{-/-}$ cells after irradiation. Increased radiosensitivity of other tissues, such as immune cells and hair follicles was also detected in Fus1$^{-/-}$ mice. Our findings demonstrate a previously unknown radioprotective function of the mitochondrial tumor suppressor Fus1 in normal tissues and suggest new individualized therapeutic approaches based on Fus1 expression.

About 50% of current cancer patients receive ionizing radiation (IR) therapy.[1] Although tumors can develop or have intrinsic radioresistance, the primary limitation of radiation therapy is tolerance of normal tissues. In particular, the well-described gastrointestinal (GI) syndrome is the major factor limiting efficacy of therapy of abdominal and pelvic cancers.[2–4] Strategies to improve radiation therapy can include increasing sensitivity of tumor cells and/or increasing resistance of normal tissues. These strategies will be accelerated by understanding drivers of tissue response to IR that can be correlated with the specific genetic background of individual patients.[5]

Response to radiation has been extensively investigated and is a linchpin of cancer therapy for many solid tumors. However, molecular mechanisms determining normal tissue response to radiation are poorly understood. Specifically, identification of new genetic factors involved in radiation response is critical for understanding inter-patient variability and improvement of individualized cancer therapy. This patient-to-patient variability is a complex polygenic trait that results from the interaction of a number of genes in different cellular pathways.[6,7] Several knockout mouse models for p53 and its targets,[8–12] NFκB[13] and other genes[14] have identified some of the molecular mechanisms driving cellular, tissue, and organismal response to radiation. However, additional critical mechanisms contributing to radiation response remain to be defined.

We previously found that deficiency of mitochondrial tumor suppressor Fus1 results in multiple immune system defects, perturbed inflammatory response, aberrant cytokine expression, as well as dysregulation of mitochondrial homeostasis including generation of high levels of ROS.[15,16] Fus1 expression is epigenetically suppressed by asbestos exposure[17,16] and tobacco smoking,[18,19] demonstrating that inhibition of Fus1 expression can occur in normal tissues under chronic oxidative stress. These findings suggest that individuals with chronic oxidative stress may have low Fus1 levels and hence become more sensitive to the side effects of radiation therapy.

On the other hand, the fact that Fus1 expression is decreased or lost in majority of lung and many head-and-neck, breast and kidney cancers may render these tumors

[1]Department of Medicine, Division of Nephrology, Vanderbilt University, Nashville, TN 37232, USA; [2] Vanderbilt-Ingram Cancer Center, Vanderbilt University, Nashville, TN 37232, USA; [3]Meharry Medical College, Department of Biochemistry and Cancer Biology, Nashville, TN, 37208, USA; [4]Department of Surgery, Division of Otolaryngology, Yale School of Medicine, New Haven, CT 06510, USA; [5]Yale Cancer Center, New Haven, CT, USA and [6]Department of Pathology, Yale School of Medicine, New Haven, CT, USA

*Corresponding author: AV Ivanova, Department of Surgery, Division of Otolaryngology, Yale School of Medicine, 333 Cedar Street, BML 231, New Haven, CT 06510, USA. Tel: +20 3785 6329; Fax: +20 3737 6425; E-mail: alla.ivanova@yale.edu

more sensitive to IR therapy.[17–19] Therefore, Fus1 may have an important role in the regulation of cellular radiosensitivity/radioresistance in normal and tumor tissues as well as be a prospective target for therapies that better balance risks and benefits of radiation treatment of tumors.

In this study, we demonstrated that whole-body irradiation (WBI) of Fus1$^{-/-}$ mice resulted in increased and accelerated death likely driven by accelerated apoptosis and untimely reentry into cell cycle, leading to mitotic catastrophe of crypt epithelial cells and diminished crypt regeneration. Study of the molecular mechanisms associated with the absence of Fus1 expression demonstrated alterations in the key signaling pathways regulating apoptosis, cell cycle, DNA repair, and oxidative stress response in irradiated GI epithelium. Lack of Fus1 was also associated with similar IR-induced defects in immune cells and hair follicles, suggesting that effects of Fus1 loss are not restricted to GI mucosa. Our findings describe Fus1 as a modulator of oxidative stress and radiosensitivity and provide a foundation for developing new individualized therapeutic approaches based on Fus1 expression, which will help balancing radiotherapy of tumors with protection of normal tissues.

Results

Fus1 protects mice from radiation-induced death. Survivals of Fus1 WT and Fus1 KO mice were compared following WBI with 8, 9 or 10 Gy. Upon WBI, survival of both Fus1$^{+/+}$ and Fus1$^{-/-}$ mice was dose-dependent; however, based on survival rate and survival time after irradiation, Fus1$^{-/-}$ mice were more sensitive than Fus1$^{+/+}$ mice (Figure 1a). Remarkably, 30% of Fus1$^{-/-}$ mice succumbed to 8 Gy WBI, typically a non-lethal dose for WT mice. To determine if the absence of Fus1 altered latency of death after WBI, higher doses of 9 and 10 Gy that cause high rates of lethality in WT mice were used. At both doses, Fus1$^{-/-}$ mice died earlier than Fus1$^{+/+}$ mice (Figure 1a). In addition, 9 Gy resulted in 100% mortality in Fus1$^{-/-}$ mice at day 12 after WBI, but allowed for 15% of Fus1$^{+/+}$ mice to survive at day 18. The dynamics of daily weight loss following 9 Gy of WBI suggested that mice were dying from the GI syndrome (Figure 1b). Supporting this suggestion, irradiated Fus1 KO mice had increased severe diarrhea and stomach bleeding.

Fus1 KO mice showed increased apoptosis in GI epithelium at 4 and 8 h post IR. To better define the role of Fus1 in regulating the dynamics of GI damage in response to IR, small intestine (jejunum and ileum) from WT and Fus1 KO mice were examined after high doses of WBI using histopathological (hematoxylin and eosin (H&E) staining) and immunohistochemical analyses. At 4 and 8 h after irradiation with 12 Gy, apoptotic cells were identified by TUNEL staining. Compared with WT mice, the crypt epithelium in Fus1$^{-/-}$ mice displayed statistically significant increase in apoptosis at 4 and 8 h post IR (Figure 2; apoptotic cells/crypt WT *versus* KO, 4 h post IR: 3.54 ± 0.90 *versus* 6.30 ± 0.49, $P = 0.028$; 8 h post IR 5.48 ± 1.07 *versus* 11.84 ± 0.63, $P < 0.001$).

Untimely proliferation in small intestine from Fus1 KO mice at 8 h post IR correlates with increased aberrant mitoses rate and rapid death of crypt cells. After high IR
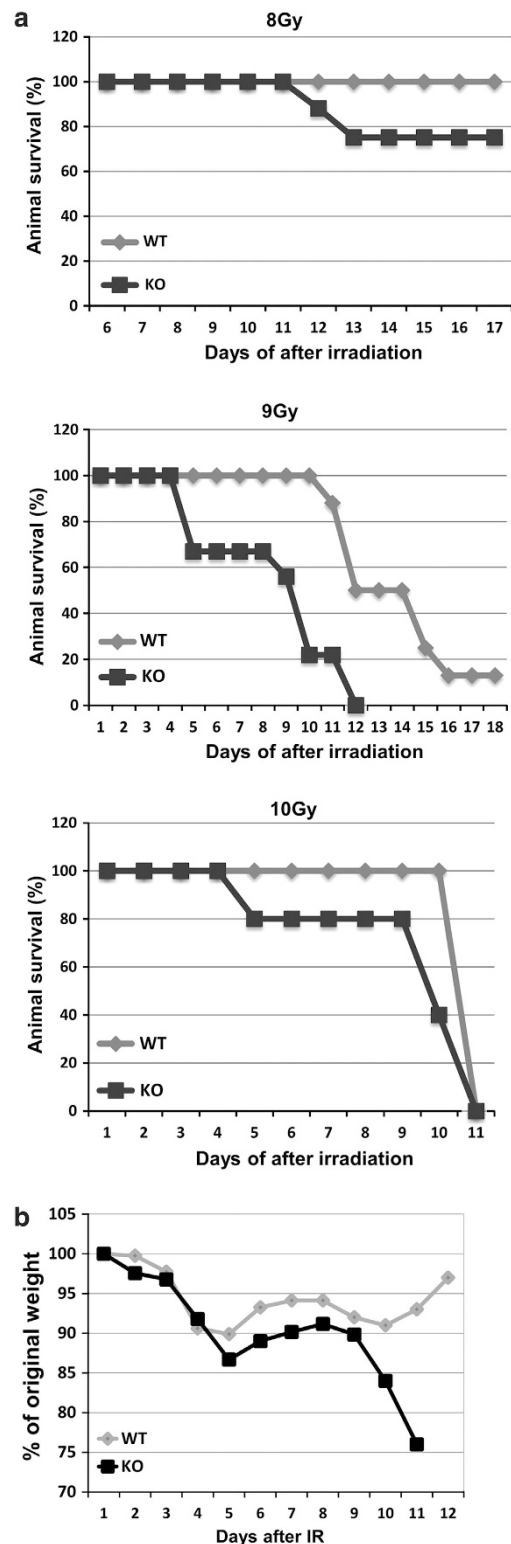
Figure 1 Effect of Fus1 deficiency on mouse survival after exposure to different doses of WBI. Fus1 WT and Fus1 KO female mice (5–6 weeks of age, 6–10 animals per group) were exposed to 8, 9 and 10 Gy WBI. Mice were weighed daily and observed for the signs of pre-morbid state. Shown are Kaplan–Meier survival curves (**a**) and graphs of the average animal weight for 9 Gy (**b**)
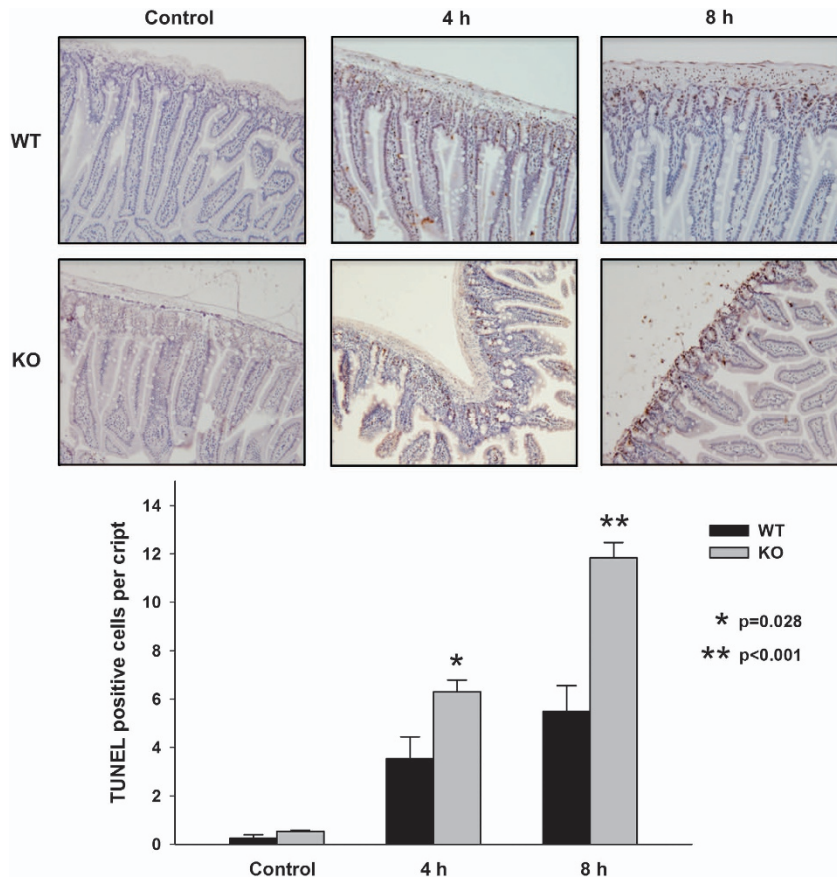
Figure 2 Apoptosis in Fus1$^{+/+}$ and Fus1$^{-/-}$ intestinal crypts after 12 Gy WBI. Sections of distal jejunum from sham-irradiated and irradiated WT and Fus1 KO mice at 4 and 8 h post IR were prepared and assayed with TUNEL staining. Shown is a bar graph of the average numbers of TUNEL-positive (apoptotic) cells per crypt in each treatment group with SEM from at least three mice in each group, 50 crypts per mouse

doses, epithelial cells in the GI crypts enter a reversible prolonged G1 cell cycle arrest that is thought to be important for repair of damaged DNA before DNA synthesis and mitosis.[20] To determine if loss of Fus1 abrogates these cell cycle checkpoints, cellular proliferation in GI crypts was examined at 4, 8, and 24 h after 12 Gy WBI (Figure 3a). While no difference between Fus1 WT and KO mice was observed at 4 h post IR (Figure 3a; proliferating cells/crypt: WT 5.3 ± 0.55 versus KO 4.72 ± 0.61, P = 0.5), a statistically significant increase in the amount of proliferating cells occurred in Fus1$^{-/-}$ mice at 8 h post IR (Figure 3a; proliferating cells/crypt: WT 4.6 ± 0.55 versus KO, 7.26 ± 0.38, P = 0.01). Interestingly, at 24 h after WBI, a trend toward decreased proliferation was observed in Fus1$^{-/-}$ crypts (Figure 3a; proliferating cells/crypt: WT, 3.03 ± 0.16 versus 2.06 ± 0.3, P = 0.07). Together, these data suggest that, like cells from WT mice, Fus1$^{-/-}$ GI crypt cells undergo a growth arrest after high-dose irradiation. Unlike GI cells from WT mice that undergo a prolonged growth arrest lasting at least 24 h, cells from Fus1$^{-/-}$ mice reenter the cell cycle as soon as 8 h after high-dose WBI (Figure 3a). The sharp decrease in Fus1 KO cell proliferation at 24 h post IR may be explained by a re-initiation of cell cycle arrest or by death of cells that prematurely entered the cell

cycle and did not have sufficient time to repair IR-induced DNA damage. Analyses of mitoses in GI cells from Fus1 WT and KO mice at 24 h post IR, revealed a two-fold decrease in the number of normal mitoses (WT, 0.025 ± 0.007 versus KO 0.01 ± 0.002, P < 0.05) and a more than three-fold increase in abnormal mitoses in Fus1$^{-/-}$ crypts (WT, 0.064 ± 0.025 versus KO, 0.238 ± 0.035, P < 0.01) (Figures 3b and c).

Fus1 KO mice show impaired crypt regeneration at 72 and 96 h post IR. It is well established that WBI with doses of >8 Gy induces cell cycle arrest and apoptosis of GI crypt epithelial cells within 24 h, leading to a decrease in regenerating crypt colonies by day 3.5 and associated crypt depletion.[21] As Fus1 loss altered crypt cell proliferation and apoptosis at early time points (Figures 2 and 3), we examined effects of Fus1 loss on the morphology of jejunum epithelia for various time points over a period of 4 days after irradiation with 12 Gy. At early time points post IR (<24 h), when differences in crypt cell apoptosis and proliferation were observed, crypt morphology of WT and Fus1 KO mice was similar; however, at later time points, dramatic differences in jejunal crypt morphology and regeneration were detected (Figure 4). At 48 h post IR, crypt size and cell counts were decreased in mice of both genotypes; however,
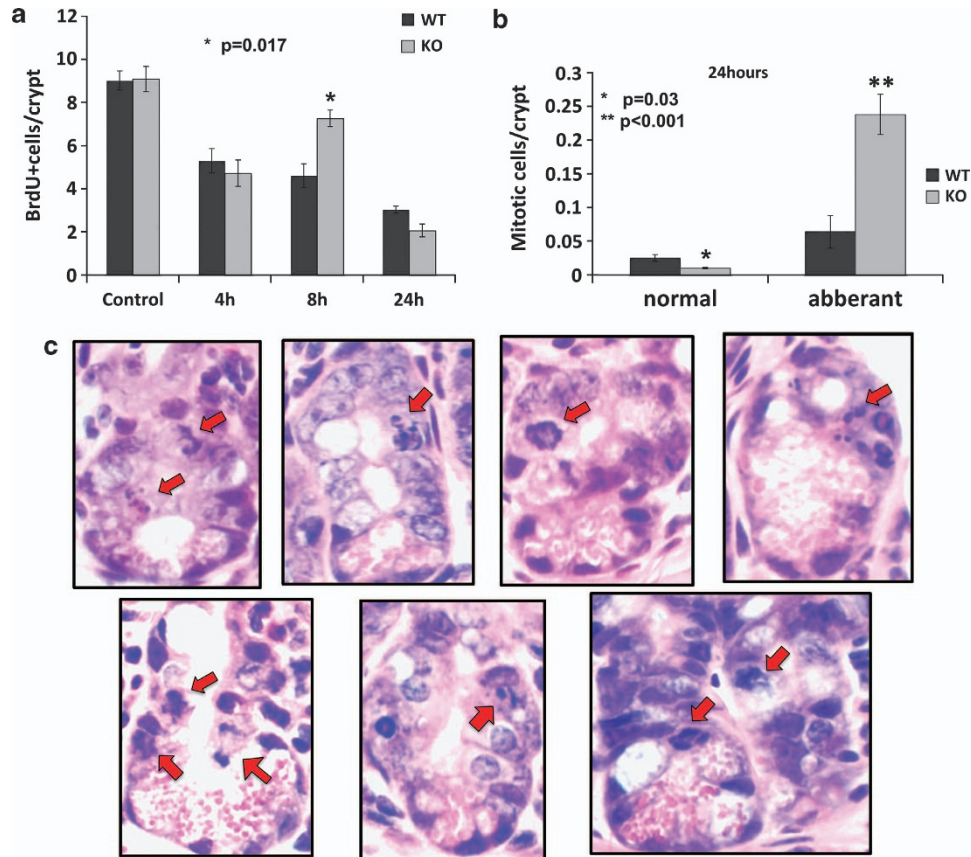
Figure 3 Proliferation and aberrant mitosis in Fus1$^{+/+}$ and Fus1$^{-/-}$ intestinal crypts after 12 Gy WBI. (**a**) Sections of distal jejunum from BrdU-injected sham-irradiated and irradiated WT and Fus1 KO mice at different time points after irradiation were prepared and stained with anti-BrdU. Shown is a bar graphs of the average numbers of BrdU-positive proliferating cells per crypt in each treatment group with S.E.M. from at least three mice in each group, 100 half-crypt sections per mouse. (**b** and **c**) Sections of distal jejunum from sham-irradiated and irradiated WT and Fus1 KO mice at 24 h post IR were prepared and stained with H&E. Shown is a bar graphs of the average numbers of cells with normal and aberrant mitoses per crypt in each treatment group with S.E.M. from at least three mice in each group, 100 half-crypt sections per mouse (**b**). Shown are micrographs of half-crypts with aberrant mitoses from Fus1$^{-/-}$ jejunum at 24 h post IR indicated by red arrows (× 400 magnification) (**c**)

at 72 h after IR, Fus1$^{+/+}$, but not Fus1$^{-/-}$ jejuna revealed regenerating crypts, as indicated by morphology (Figure 4a). Loss of crypts in Fus1$^{-/-}$ mice was accompanied by morphological deterioration of villi epithelia, with progression to complete degeneration at 96 h post IR. Although at 96 h time point occasional regenerating crypts could be found in Fus1$^{-/-}$ jejunum, they demonstrated altered morphology, size and proliferation rates, and were enriched with aberrant mitoses when compared to regenerating crypts from WT mice (Figures 4b–d). As almost all crypts vanished between 48 and 72 h post IR in both WT and KO mice, the crypts found at 96 h time point are likely to be formed *de novo*, being derived from stem cells that re-establish proliferative capacity. These data suggest that in the absence of Fus1, stem cells cannot repopulate crypts after damage by high dose of IR, implying that Fus1 may protect crypt epithelia stem cells from IR damage.

Activation of early radiation response markers in mucosa of Fus1 KO mice is altered. To compare molecular events occurring in GI epithelial cells early after IR, we isolated small intestinal mucosa cells from Fus1$^{+/+}$ and Fus1$^{-/-}$ mice at 0, 4 and 8 h after treatment with 12 Gy

WBI, and activation/expression of IR apoptosis/injury response regulators was examined by immunoblotting. At 4 h post IR, in Fus1$^{-/-}$ cells, we found increased phosphorylation of histone H2AX at serine 139 (γ-H2AX), activation of GSK-3β (decreased inactivating phosphorylation at serine 9), and accumulation of apoptotic markers such as Bax and cleaved PARP1 (Figure 5). In agreement with increased numbers of apoptotic cells seen in Fus1$^{-/-}$ compared to Fus1$^{+/+}$ crypts at 4 and 8 h after IR (Figure 2), cleaved PARP1 was much higher at 4 h, and Bax was increased at 4 and 8 h post IR (Figure 5). Remarkably, absence of Fus1 was associated with a marked decrease in γH2AX along with total H2AX and an increase in inhibitory phosphorylation of GSK-3β at 8 h post IR, suggesting that Fus1 regulates phosphorylation of these proteins after IR (Figure 5).

Fus1$^{-/-}$ epithelial cells are defective in early and late response to IR. Fus1 deficiency resulted in aberrant cellular and tissue response, as well as molecular response in mice exposed to 12 Gy WBI. To further characterize the role of Fus1 during early radiation response, we used spontaneously immortalized Fus1$^{+/+}$ and Fus1$^{-/-}$ murine epithelial cells. We applied *in vitro* system for expanded studying of
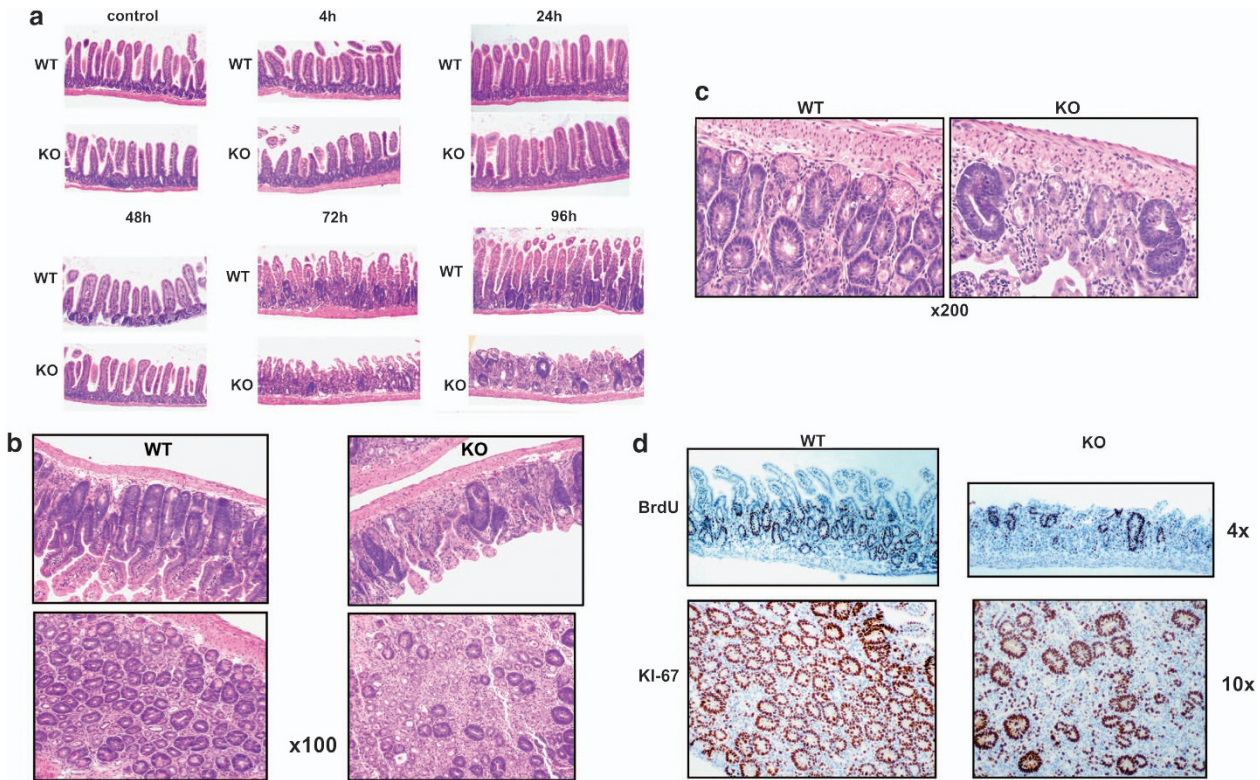
Figure 4 Dynamics of radiation injury and regeneration in small intestines of Fus1$^{+/+}$ and Fus1$^{-/-}$ mice after irradiation with 12 Gy WBI. (**a–c**) Shown are micrographs of H&E-stained paraffin sections of small intestines from sham-irradiated and irradiated Fus1 WT and Fus1 KO mice. (**a**) Time after IR 0–96 h; $\times 40$ magnification. (**b**) Time after IR 96 h; $\times 100$ magnification. (**c**) Time after IR 96 h; $\times 200$ magnification (**d**) Shown are micrographs of paraffin sections of small intestines from sham-irradiated and irradiated Fus1 WT and Fus1 KO BrdU-injected mice stained for BrdU incorporation (upper panel) and proliferative marker Ki67 (lower panel)

IR-response pathways affected by Fus1 loss to complement the data obtained in mouse tissues. This approach allowed overcoming the technical difficulties of working with non-homogenous animal tissues. Moreover, we utilized the benefit of cultured cells to characterize Fus1-dependent early radiation response (0.5–2 h after exposure). Cells were irradiated with 9 Gy, and lysates were examined by immunoblotting during the early (0 to 8 h) post-IR phase. Dynamics of critical IR-response proteins representing cell cycle, proliferation, DNA damage and repair, signal transduction, and oxidative stress response molecular pathways were investigated (Figure 6). We found that the basal levels of signal transduction proteins GSK-3β (total and phosphorylated), phospho-p38 (Figure 6b) and anti-oxidant protein PRDX1 (Figure 6c) were higher in Fus1$^{-/-}$ cells. These data are consistent with known consequences of Fus1 deficiency associated with chronic oxidative stress and deregulated signaling pathways. We also observed a pronounced Fus1-dependent difference in the dynamics of IR response: while in WT cells, activation of most of the analyzed molecules was steadily increasing during early post-IR time points, in Fus1 KO cells, we observed a biphasic IR response pattern. In Fus1$^{+/+}$ cells, majority of investigated proteins were activated between 30 min and 1 h (Figure 6: increased activating phosphorylation of p53, NfκB and p38; accumulation of p53, NfκB, cyclins B1 and D1, PRDX1, and SOD2), while Fus1$^{-/-}$ cells showed no or low response to radiation

damage between 0 and 2 h post IR. Moreover, the 1-h time point appeared critical for the survival of Fus1$^{-/-}$ cells, as at this time, the levels of nearly all early-response markers dropped to the basal level. Noteworthy, after this critical point, Fus1$^{-/-}$ cells entered the second phase of IR response. Specifically, they showed a sharp increase in the activation of majority of analyzed markers at 2 h post IR (Figures 6a–c, increased activating phosphorylation of NFκB and ERK1/2; accumulation of NfκB, cyclin D1, and SOD2). Interestingly, three proteins, p53, GSK-3β and p38, unlike other IR response proteins in Fus1$^{-/-}$ cells, demonstrated a strong change in activity as early as 30 min post IR and at much higher levels than in Fus1$^{+/+}$ cell. Although the p53 response, as measured by phosphorylation and accumulation, was greater in Fus1$^{-/-}$ cells, the time course of p53 activation was similar in WT and Fus1$^{-/-}$ cells (Figure 6a). In contrast, the pattern and extent of phosphorylation of p38 (activating) and GSK-3β (inhibiting) was distinct in Fus1 KO cells (Figure 6b). In WT cells, p38 phosphorylation increased moderately for the first hour after IR and rapidly decreased to below the basal level at 2 h after treatment (Figure 6b). In contrast, irradiation of Fus1$^{-/-}$ cells resulted in high levels of p38 phosphorylation at 30 min followed by a decrease at 1 h, then a second wave of phosphorylation at 2 h post IR followed by a decrease to below levels seen in sham-irradiated cells at 8 h (Figure 6b). Inhibiting phosphorylation of GSK-3β in Fus1$^{-/-}$ cells demonstrated a similar biphasic
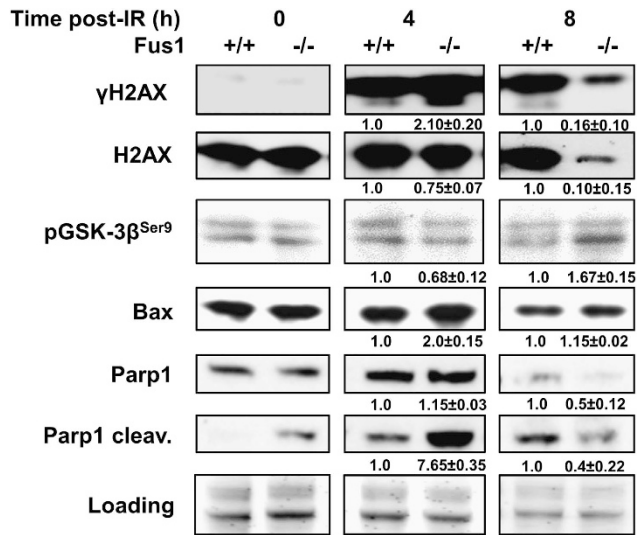
6

Figure 5 Dynamics of molecular radiation-induced changes in mucosa of Fus1 WT and Fus1KO mice. GI mucosa cells were isolated from WT and Fus1 KO mice irradiated with 12 Gy at 0, 4 and 8 h post IR. Shown are western immunoblot analyses using antibodies against DNA damage and apoptotic proteins. Membrane staining for total protein/well was used as a loading control. Average relative fold change in protein levels with SEM is shown (number of analyzed mice per group is 3)

pattern with initial phosphorylation at 30 min after IR, followed by decreased phosphorylation at 1 h and a second wave of phosphorylation beginning at 2 h post IR (Figure 6b). However, unlike for p38, phosphorylation of GSK-3β continued to increase throughout all experimental time points (Figure 6b).

Discussion

In this study, we identified the mitochondrial tumor suppressor Fus1 as a novel factor involved in the protection of radio-sensitive cells of the GI tract and other organs against IR damage. Upon WBI, Fus1 KO mice demonstrated decreased survival due to accelerated GI syndrome, as compared with WT mice. Fus1 KO GI crypt epithelial cells underwent a short period of IR-induced proliferative arrest followed either by apoptosis or by rapid proliferation without sufficient time for DNA repair. This abnormality resulted in the increased number of aberrant mitoses, death of crypt cells and massive crypt loss. Moreover, individual crypts that attempted to regenerate displayed abnormal morphology. Interestingly, the events leading to compromised crypt regeneration in Fus1 KO mice were similar to the IR-induced cellular events observed in other mouse models of radiosensitivity, such as p53- and p21-deficient mice[8,11,12,22], suggesting commonality of signaling pathways involved in response to IR.

Molecular analysis of irradiated Fus1 KO GI mucosa cells showed a significantly altered activation dynamics of IR-responsive signaling pathways as compared with irradiated WT GI cells (Figure 5). The most striking Fus1-dependent difference was the early accumulation of γH2AX, suggesting earlier activation of the DNA-repair machinery due to double-strand breaks formation as well as an increased apoptosis in the Fus1-deficient GI cells.[23] Interestingly, this H2AX activation was followed by early decrease in γH2AX
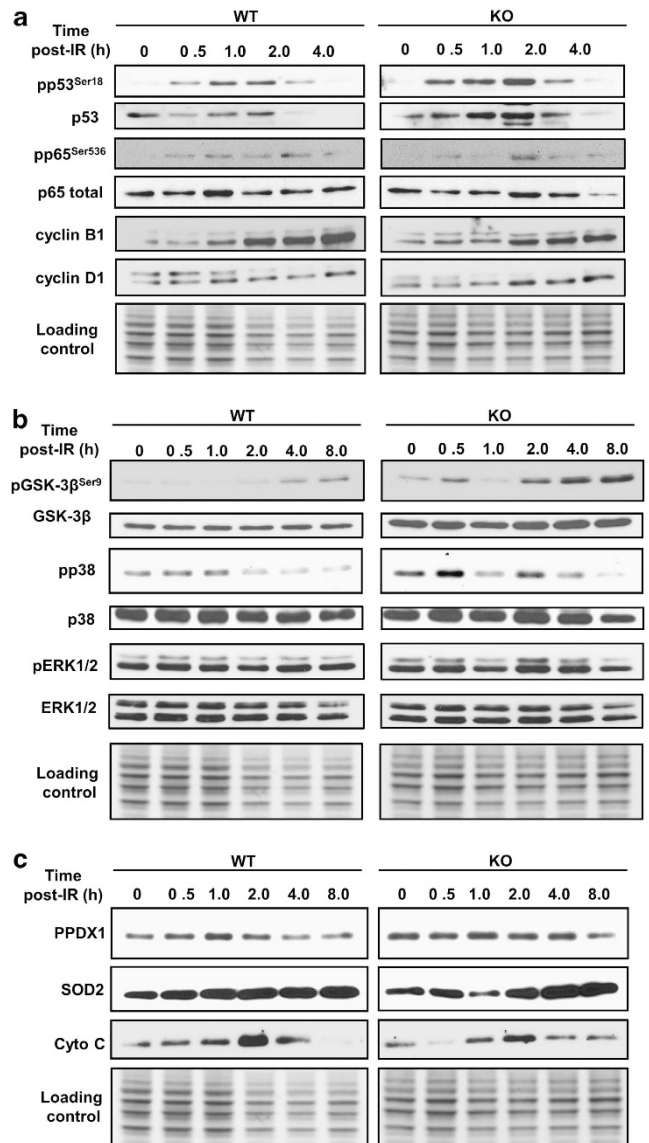

Figure 6 Dynamics of radiation-response pathways activation in Fus1$^{+/+}$ and Fus1$^{-/-}$ epithelial cells in vitro. Immortalized Fus1$^{+/+}$ and Fus1$^{-/-}$ epithelial cells were irradiated with 9 Gy and collected at several time points post IR. Shown are western immunoblot analyses for dynamics of activation of proteins from DNA damage response and apoptotic pathways (**a**), activation of signal transduction pathway proteins (**b**), activation of proteins from oxidative stress response pathways (**c**)

level (8 h post IR) that was accompanied by a dramatic decrease in total H2AX. This suggests that Fus1-dependent regulation of this protein may occur not only at the post-translational but also at the RNA/protein synthesis/degradation levels. Most important, low level of γH2AX indicates an incomplete DNA repair in Fus1$^{-/-}$ cells that may serve as the key event promoting cell death in the form of 'mitotic catastrophe' associated with aberrant mitosis.

This sequence of molecular events in GI mucosa was supported by the kinetics of accumulation of pro-apoptotic markers, cleaved PARP1 and Bax,[24] and altered activity of GSK-3β, which contributes to p53 and Bcl-2 family-mediated pro-apoptotic signaling.[25–28] The early increase in GSK-3β

activity and levels of Bax and cleaved PARP1 in the Fus1$^{-/-}$ mucosa (Figure 5) are in line with the increased apoptosis in the crypts of Fus1 KO mice at 4 and 8 h post IR as compared with the WT mucosa (Figure 2). These data suggest that radiation-induced apoptosis in intestinal epithelial cells involves, in addition to Fus1, the Bax/PARP1 pathway and that GSK-3β regulates activation of this pathway.

A more detailed analysis of Fus1-dependent molecular events in the early IR response using immortalized cultured epithelial cells (Figure 6) demonstrated involvement of compensatory p53-dependent mechanisms, which can protect Fus1-deficient cells via tight regulation of the cell cycle.[10,22] Increased early accumulation of cyclin D1 concomitant with decreased accumulation of cyclin B1 in Fus1$^{-/-}$ cells supports compensatory changes in the IR-induced cell cycle arrest. High level of cyclin D1 parallels the decreased activity of GSK-3β, suggesting that cyclin D1 accumulation is regulated by GSK-3β. This suggestion is consistent with the reports that GSK-3β-dependent phosphorylation of cyclin D1 regulates its proteolytic turnover.[29]

In our earlier studies, we demonstrated that Fus1$^{-/-}$ immune and epithelial cells produce significantly higher levels of basal and stress-induced mitochondrial ROS and experience chronic oxidative stress.[16] Mitochondria are the major source of ROS[30] that may trigger ROS-associated radiation-induced genomic instability.[31–36] Free radicals, in particular, hydroxyl radical (HO•), are highly reactive molecules. Excessive HO• formation can result in considerable damage to cellular macromolecules via lipid peroxidation within membranes, oxidative modification or fragmentation of proteins, and DNA damage.[37] IR induces formation of HO• primarily via radiolysis of water. High basal levels of HO• and other ROS in Fus1$^{-/-}$ cells can contribute to activation of p53[16,38] and early IR response markers, such as NfκB/p65, H2AX, and PARP1, as well as markers of oxidative stress and DNA damage, such as NfκB, H2AX, PARP1, ERK1/2, p38, SOD2, and cytochrome c.[39–42]

IR induces activation of cellular anti-oxidant defense mechanisms including overexpression of SOD2[43] and PRDX1.[44] Cytochrome c, which is traditionally considered a pro-apoptotic protein,[45] was recently shown to also have an anti-oxidant function.[45–48] In this study, we demonstrated that expression of cytochrome c and anti-oxidant defense proteins, PRDX1 and SOD2, are dysregulated in Fus1$^{-/-}$ epithelial cells (Figure 6). While Fus1$^{+/+}$ cells demonstrated increased PRDX1 expression in response to IR, Fus1$^{-/-}$ cells were not capable of doing so, most likely due to the already high basal level of PRDX1. SOD2 and cytochrome c also demonstrated a perturbed accumulation kinetics during early radiation response in Fus1$^{-/-}$ epithelial cells as compared with that in Fus1$^{+/+}$ cells. Therefore, we suggest that the unchanged level of PRDX1, moderate increase in cytochrome c, and delayed accumulation of SOD2 after IR resulted in inefficient response to IR-induced oxidative stress in Fus1$^{-/-}$ cells.

We have previously demonstrated that Fus1$^{-/-}$ immune and epithelial cells are characterized by dysregulated mitochondrial membrane potential (MMP). In these cells, MMP was higher in the steady state and increased dramatically under the genotoxic stress.[16] MMP has also been shown

to correlate positively with cell radiosensitivity.[49] Thus, we suggest that dysregulation of mitochondrial homeostasis including elevated intrinsic generation of ROS, increase in MMP, and inhibition of anti-oxidant defenses in Fus1$^{-/-}$ crypt epithelial cells are major contributing factors to the mechanism of radiosensitivity of Fus1 KO mice.

It is noteworthy that Fus1 also protects other radiation-sensitive tissues against damaging IR effects, specifically immune organs and hair follicles (see Supplementary Figures S1 and S2). As damage to hematopoietic system occurs concomitantly with the GI syndrome after 8–20 Gy WBI,[50,51] we analyzed the dynamics of damage to immune organs in Fus1 KO and WT mice. One of the characteristic signs of immune system damage after acute IR is depletion/atrophy of thymus and spleen. Compared with WT mice, depletion of immune cells in Fus1 KO mice was augmented in both spleen and thymus (Supplementary Figure S1).

Irradiated Fus1$^{-/-}$ mice also exhibited premature hair graying. It was observed in 100% of surviving Fus1 KO mice at 8 weeks after IR but not in WT mice (Supplementary Figure S2). Hair graying is caused by defective renewal of melanocyte stem cells,[52] a process that can be dramatically accelerated by DNA-damaging IR that abrogates their renewal.[53,54] Thus, Fus1 modulates radioresistance in cells of the GI tract, immune cells as well as melanocyte stem cells of hair follicles.

We propose the following mechanism of Fus1-dependent radioresistance (Figure 7). We have previously shown that Fus1 is responsible for the maintenance of mitochondrial homeostasis. In our current study, the response of Fus1 KO mice to IR is dysregulated compared with WT mice. Therefore, we suggest that Fus1 is a key regulator of the response to oxidative and genotoxic stress. Specifically, Fus1$^{-/-}$ cells undergo accelerated cell cycle arrest, which results in either early apoptosis or entrance into the DNA repair phase (Figure 7). However, these cells prematurely resume cell
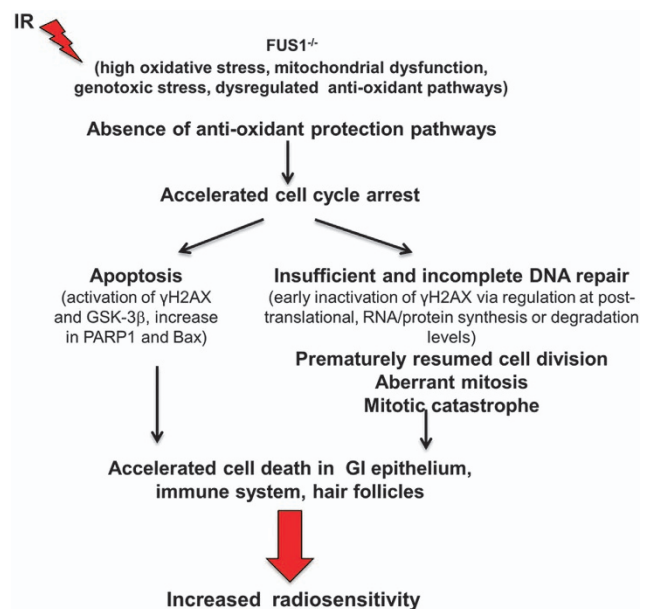

Figure 7 Schematic representation of the molecular mechanisms, cellular events and systematic response of Fus1-dependent radioprotection

division and, thus, cannot complete DNA repair, which leads to aberrant mitosis and cell death due to the mitotic catastrophe (Figure 7). These events result in accelerated cell death in GI epithelium, immune system, and hair follicles, thus signifying radiosensitive phenotype of Fus1 KO mice (Figure 7).

Traditionally, a role of tumor suppressors in disorders associated with radiosensitivity was viewed in light of molecular mechanisms underlying emergence and repair of DNA double-strand breaks.[55] The existing mouse models of radiosensitivity utilize knockout of tumor-suppressor proteins involved in cell cycle regulation and DNA repair such as p53, ataxia-telangiectasia (ATM), Nijmegen breakage syndrome (NBS), and DNA-PKcs.[55] Here, we demonstrate for the first time that tumor suppressor Fus1 modulates radiosensitivity of normal tissues via regulation of anti-oxidant response pathways.

Materials and Methods

Mouse model and irradiation. Fus1 KO mice generated by Dr. A Ivanova[15] were backcrossed to 129sv background in the laboratory of Dr. S Anderson (NCI-Frederick). All animal experiments were performed according to a protocol approved by the Institutional Animal Care and Use Committee. The mice were fed with a standard diet. The animals were housed four per cage in standard cages and under a light cycle of 12 h light–dark. They had *ad libitum* access to drinking water and normal diet throughout the experiment. WBI of mice was carried out in a Mark I 137Cs irradiator (J.L. Shepherd & Associates, San Fernando, CA, USA) at a dose rate of 167 cGy/min and total doses of 8, 9, 10 or 12 Gy. Female mice (5–6 weeks old) were irradiated in a holder designed to immobilize unanesthetized mice, as previously described.[56,57] Sham-irradiated mice were handled the same way as irradiated animals with the exception of irradiation. Experimental groups consisted of at least six animals.

Proliferation evaluation in mouse small intestine. Mice exposed to 12 Gy WBI were killed at 4, 8, 24, 48, 72 and 96 h after treatment. All mice were i.p. injected with 120 mg/kg BrdU 2 h before being killed. The proximal jejunum and distal ileum were fixed for histology in 10% formalin with PBS. For estimation of proliferation, tissues were stained with anti-KI-67 and anti-BrdU antibodies and visualized with DAB. Proliferation was scored by light microscopy analysis (Ki-67 and BrdU) in 100 half-crypt sections per mouse with at least three mice in each group. All crypts were at least 20 cells in height, with cell position 1 located at the crypt base.

TUNEL staining for GI epithelial apoptosis. Sections of proximal small intestine (6 cm distal to the stomach) and distal small intestine (2 cm proximal to the cecum) were stained with H&E. Tissue sections were stained as described previously.[56,57] The mean number of TUNEL-positive cells per crypt and standard error of the mean (S.E.M.) were calculated from 50 crypts in each treatment group consisting of at least three mice. Crypts were identified by the presence of defined Paneth cells and ⩾10 healthy-looking chromophilic non-Paneth cells.[58]

Crypt regeneration. For crypt-regeneration studies, mice were killed at 0, 4, 8, 24, 48, 72 and 96 h after 12 Gy WBI. Each mouse received i.p. injection of 120 mg/kg BrdU and was killed 2 h later. Proximal jejunum and distal ileum were fixed. Cells incorporating BrdU were detected by mouse anti-BrdU antibody, visualized by DAB (brown) and counterstained with hematoxylin (blue). A surviving crypt was defined as containing five or more adjacent chromophilic BrdU-positive non-Paneth cells, at least one Paneth cell and a lumen.

Scoring aberrant mitosis in crypt epithelial cells. At 24 h after WBI, intestines were collected and processed as described above. Crypts that were cut longitudinally so that Paneth cells and an adjacent villus could be visualized were scored for mitotic cells by a single observer blinded to genotype and treatment. Normal mitoses were scored when a cell was undergoing mitosis and the chromosomes aligned symmetrically. Aberrant mitoses were scored when chromosomes were misaligned, lagged, showed anaphase bridges or if micro-nuclei were present.[12,11]

Isolation of GI epithelial cells. For the isolation of GI epithelial cells, the small intestines from sham-irradiated and irradiated Fus1 WT and KO mice were placed in ice-cold PBS and ice-cold PBS was flushed through the intestines using a syringe. The intestines were then cut longitudinally with scissors and rinsed with cold PBS. The small intestines were placed in PBS with 3 mM EDTA and 50 mM DTT, and stored on ice for 1 h in 50-ml conical tubes. Then, the tubes were shaken 15 times to detach the GI epithelia. The muscularis was removed and the GI epithelia were collected by centrifugation. The cells were washed with PBS, lysed in 2 × Laemmi sample buffer and subjected to western immunoblot analysis.

Fus1 WT and KO immortalized epithelial cells. Primary normal epithelial cells were obtained from Fus1 WT and Fus1 KO mice by trypsinization of small tissue pieces for 15 min at 37 °C. Trypsinized cells were re-suspended in 10% FBS/DMEM high glucose medium, plated and maintained in culture for 4 months with regular (2–3 times a week) re-plating until the cells immortalized spontaneously. For irradiation, cells were routinely cultured till 70–80% confluency and then exposed to 9 Gy IR using Mark I 137Cs irradiator. Cells were returned to tissue-culture incubator and lysed at 0, 0.5, 1, 2, 4, and 8 h post irradiation using M-PER kit (Thermo Fisher Scientific, Rockford, IL, USA). Protein concentration was quantified using BCA reagent (Thermo Fisher Scientific). Protein extracts (100 μg) were subjected to western immunoblot analysis.

Western immunoblot analysis. Western immunoblot analysis was performed using antibodies against the following proteins: H2AX (Abcam, Cambridge, MA, USA), γH2AX (Abcam), PARP1 (Santa Cruz Biotechnology, Inc., Dallas, TX, USA), PRDX1 (Sigma-Aldrich, St. Louis, MO, USA), SOD2 (R&D Systems, Inc., Minneapolis, MN, USA), Cytochrome c (Santa Cruz Biotechnology, Inc.), NF-κB p65, phospho-p65^{Ser536}, p53, phospho-p53^{Ser18}, Cyclin B1, Cyclin D1, GSK-3β, phospho-GSK-3β^{Ser9}, ERK1/2, phospho-ERK1/2$^{Thr202/Tyr204}$, p38, phospho-p38$^{Thr180/Tyr182}$ (all from Cell Signaling Technologies, Danvers, MA, USA). The band intensity was determined using ImageJ software, normalized to loading control and presented as a relative fold change (WT/KO).

Statistical analysis. Student's *t*-test was used to compare two groups and one-way analysis of variance (ANOVA) and Holm–Sidak multiple-group post-test comparisons was used for comparisons among multiple groups. All statistical tests were two-sided and statistical analysis was done with the use of SigmaStat software (Systat Software Inc., San Jose, CA, USA). Statistical significance was defined as $P < 0.05$. Data are presented as means with S.E.M.

Conflict of Interest
The authors declare no conflict of interest.

Author Contributions
EMY designed the research, performed the experiments, analyzed the data, and wrote the manuscript; R.U. performed the experiments, analyzed the data; PAV analyzed the data, consulted and wrote the manuscript, WGY analyzed the data, consulted and helped with the manuscript preparation, AVI designed the research, performed the experiments, analyzed the data, and wrote the manuscript.

Disclaimer
The sponsors had no involvement in the design of the study; the collection, analysis, and interpretation of the data; the writing of the manuscript; or the decision to submit the manuscript for publication.

1. Delaney G, Jacob S, Featherstone C, Barton M. The role of radiotherapy in cancer treatment: estimating optimal utilization from a review of evidence-based clinical guidelines. *Cancer* 2005; **104**: 1129–1137.
2. Gale RP. Immediate medical consequences of nuclear accidents. Lessons from Chernobyl. *JAMA* 1987; **258**: 625–628.
3. Dubois A, Walker RI. Prospects for management of gastrointestinal injury associated with the acute radiation syndrome. *Gastroenterology* 1988; **95**: 500–507.
4. Hall EJ, Giaccia AJ. *Radiobiology for the radiologist*. 6th Edn Lippincott Williams & Wilkins: Philadelphia, 2006.
5. Begg AC, Stewart FA, Vens C. Strategies to improve radiotherapy with targeted drugs. *Nature Rev* 2011; **11**: 239–253.

6. Andreassen CN, Alsner J, Overgaard J. Does variability in normal tissue reactions after radiotherapy have a genetic basis—where and how to look for it? *Radiother Oncol* 2002; **64**: 131–140.

7. Travis EL. Genetic susceptibility to late normal tissue injury. *Semin Radiat Oncol* 2007; **17**: 149–155.

8. Merritt AJ, Allen TD, Potten CS, Hickman JA. Apoptosis in small intestinal epithelial from p53-null mice: evidence for a delayed, p53-independent G2/M-associated cell death after gamma-irradiation. *Oncogene* 1997; **14**: 2759–2766.

9. Komarova EA, Kondratov RV, Wang K, Christov K, Golovkina TV, Goldblum JR et al. Dual effect of p53 on radiation sensitivity *in vivo*: p53 promotes hematopoietic injury, but protects from gastro-intestinal syndrome in mice. *Oncogene* 2004; **23**: 3265–3271.

10. Gudkov AV, Komarova EA. The role of p53 in determining sensitivity to radiotherapy. *Nat Rev Cancer* 2003; **3**: 117–129.

11. Leibowitz BJ, Qiu W, Liu H, Cheng T, Zhang L, Yu J. Uncoupling p53 functions in radiation-induced intestinal damage via PUMA and p21. *Mol Cancer Res* 9: 616–625.

12. Kirsch DG, Santiago PM, di Tomaso E, Sullivan JM, Hou WS, Dayton T et al. p53 controls radiation-induced gastrointestinal syndrome in mice independent of apoptosis. *Science* **327**: 593–596.

13. Wang Y, Meng A, Lang H, Brown SA, Konopa JL, Kindy MS et al. Activation of nuclear factor kappaB In vivo selectively protects the murine small intestine against ionizing radiation-induced damage. *Cancer Res* 2004; **64**: 6240–6246.

14. Kolesnick R, Fuks Z. Radiation and ceramide-induced apoptosis. *Oncogene* 2003; **22**: 5897–5906.

15. Ivanova AV, Ivanov SV, Pascal V, Lumsden JM, Ward JM, Morris N et al. Autoimmunity, spontaneous tumourigenesis, and IL-15 insufficiency in mice with a targeted disruption of the tumour suppressor gene Fus1. *J Pathol* 2007; **211**: 591–601.

16. Uzhachenko R, Issaeva N, Boyd K, Ivanov SV, Carbone DP, Ivanova AV. Tumour suppressor Fus1 provides a molecular link between inflammatory response and mitochondrial homeostasis. *J Pathol* 2012; **227**: 456–469.

17. Ivanova AV, Ivanov SV, Prudkin L, Nonaka D, Liu Z, Tsao A et al. Mechanisms of FUS1/TUSC2 deficiency in mesothelioma and its tumorigenic transcriptional effects. *Mol Cancer* 2009; **8**: 91.

18. Lerman MI, Minna JD. The 630-kb lung cancer homozygous deletion region on human chromosome 3p21.3: identification and evaluation of the resident candidate tumor suppressor genes. The International Lung Cancer Chromosome 3p21.3 Tumor Suppressor Gene Consortium. *Cancer Res* 2000; **60**: 6116–6133.

19. Prudkin L, Behrens C, Liu DD, Zhou X, Ozburn NC, Bekele BN et al. Loss and reduction of FUS1 protein expression is a frequent phenomenon in the pathogenesis of lung cancer. *Clin Cancer Res* 2008; **14**: 41–47.

20. Nagasawa H, Keng P, Harley R, Dahlberg W, Little JB. Relationship between gamma-ray-induced G2/M delay and cellular radiosensitivity. *Int J Radiat Biol* 1994; **66**: 373–379.

21. Potten CS, Booth C, Pritchard DM. The intestinal epithelial stem cell: the mucosal governor. *Int J Exp Pathol* 1997; **78**: 219–243.

22. Gudkov AV, Komarova EA. Pathologies associated with the p53 response. *Cold Spring Harb Perspect Biol* 2: a001180.

23. Rogakou EP, Nieves-Neira W, Boon C, Pommier Y, Bonner WM. Initiation of DNA fragmentation during apoptosis induces phosphorylation of H2AX histone at serine 139. *J Biol Chem* 2000; **275**: 9390–9395.

24. D'Amours D, Sallmann FR, Dixit VM, Poirier GG. Gain-of-function of poly(ADP-ribose) polymerase-1 upon cleavage by apoptotic proteases: implications for apoptosis. *J Cell Sci* 2001; **114**(Pt 20): 3771–3778.

25. Watcharasit P, Bijur GN, Zmijewski JW, Song L, Zmijewska A, Chen X et al. Direct, activating interaction between glycogen synthase kinase-3beta and p53 after DNA damage. *Proc Natl Acad SciUSA* 2002; **99**: 7951–7955.

26. Rotolo JA, Maj JG, Feldman R, Ren D, Haimovitz-Friedman A, Cordon-Cardo C et al. Bax and Bak do not exhibit functional redundancy in mediating radiation-induced endothelial apoptosis in the intestinal mucosa. *Int J Radiat Oncol Biol Phys* 2008; **70**: 804–815.

27. Pritchard DM, Potten CS, Korsmeyer SJ, Roberts S, Hickman JA. Damage-induced apoptosis in intestinal epithelia from bcl-2-null and bax-null mice: investigations of the mechanistic determinants of epithelial apoptosis *in vivo*. *Oncogene* 1999; **18**: 7287–7293.

28. Przemeck SM, Duckworth CA, Pritchard DM. Radiation-induced gastric epithelial apoptosis occurs in the proliferative zone and is regulated by p53, bak, bax, and bcl-2. *Am J Physiol* 2007; **292**: G620–G627.

29. Diehl JA, Cheng M, Roussel MF, Sherr CJ. Glycogen synthase kinase-3beta regulates cyclin D1 proteolysis and subcellular localization. *Genes Dev* 1998; **12**: 3499–3511.

30. Marchi S, Giorgi C, Suski JM, Agnoletto C, Bononi A, Bonora M et al. Mitochondria-ros crosstalk in the control of cell death and aging. *J Signal Transduct* 2012; **2012**: 329635.

31. Limoli CL, Kaplan MI, Corcoran J, Meyers M, Boothman DA, Morgan WF. Chromosomal instability and its relationship to other end points of genomic instability. *Cancer Res* 1997; **57**: 5557–5563.

32. Limoli CL, Kaplan MI, Giedzinski E, Morgan WF. Attenuation of radiation-induced genomic instability by free radical scavengers and cellular proliferation. *Free Radic Biol Med* 2001; **31**: 10–19.

33. Samper E, Nicholls DG, Melov S. Mitochondrial oxidative stress causes chromosomal instability of mouse embryonic fibroblasts. *Aging Cell* 2003; **2**: 277–285.

34. Liu L, Trimarchi JR, Smith PJ, Keefe DL. Mitochondrial dysfunction leads to telomere attrition and genomic instability. *Aging Cell* 2002; **1**: 40–46.

35. Kim GJ, Fiskum GM, Morgan WF. A role for mitochondrial dysfunction in perpetuating radiation-induced genomic instability. *Cancer Res* 2006; **66**: 10377–10383.

36. Kim GJ, Chandrasekaran K, Morgan WF. Mitochondrial dysfunction, persistently elevated levels of reactive oxygen species and radiation-induced genomic instability: a review. *Mutagenesis* 2006; **21**: 361–367.

37. Vanlangenakker N, Vanden Berghe T, Krysko DV, Festjens N, Vandenabeele P. Molecular mechanisms and pathophysiology of necrotic cell death. *Curr Mol Med* 2008; **8**: 207–220.

38. Lee DH, Rhee JG, Lee YJ. Reactive oxygen species up-regulate p53 and Puma; a possible mechanism for apoptosis during combined treatment with TRAIL and wogonin. *Br J Pharmacol* 2009; **157**: 1189–1202.

39. Burdelya LG, Krivokrysenko VI, Tallant TC, Strom E, Gleiberman AS, Gupta D et al. An agonist of toll-like receptor 5 has radioprotective activity in mouse and primate models. *Science* 2008; **320**: 226–230.

40. Gudkov AV, Komarova EA. Radioprotection: smart games with death. *J Clin Invest* **120**: 2270–2273.

41. Mah LJ, El-Osta A, Karagiannis TC. gammaH2AX: a sensitive molecular marker of DNA damage and repair. *Leukemia* 2010; **24**: 679–686.

42. Albert JM, Cao C, Kim KW, Willey CD, Geng L, Xiao D et al. Inhibition of poly(ADP-ribose) polymerase enhances cell death and improves tumor growth delay in irradiated lung cancer models. *Clin Cancer Res* 2007; **13**: 3033–3042.

43. Hosoki A, Yonekura S, Zhao QL, Wei ZL, Takasaki I, Tabuchi Y et al. Mitochondria-targeted superoxide dismutase (SOD2) regulates radiation resistance and radiation stress response in HeLa cells. *J Radiat Res* 2012; **53**: 58–71.

44. Chen WC, McBride WH, Iwamoto KS, Barber CL, Wang CC, Oh YT et al. Induction of radioprotective peroxiredoxin-I by ionizing irradiation. *J Neurosc Res* 2002; **70**: 794–798.

45. Huttemann M, Pecina P, Rainbolt M, Sanderson TH, Kagan VE, Samavati L et al. The multiple functions of cytochrome c and their regulation in life and death decisions of the mammalian cell: From respiration to apoptosis. *Mitochondrion* 2011; **11**: 369–381.

46. Pereverzev MO, Vygodina TV, Konstantinov AA, Skulachev VP. Cytochrome c, an ideal antioxidant. *Biochem Soc Transact* 2003; **31**(Pt 6): 1312–1315.

47. Pepelina TY, Chertkova RV, Ostroverkhova TV, Dolgikh DA, Kirpichnikov MP, Grivennikova VG et al. Site-directed mutagenesis of cytochrome c: reactions with respiratory chain components and superoxide radical. *Biochemistry (Mosc)* 2009; **74**: 625–632.

48. Velayutham M, Hemann C, Zweier JL. Removal of H(2)O(2) and generation of superoxide radical: role of cytochrome c and NADH. *Free Radic Biol Med* 2011; **51**: 160–170.

49. Harper ME, Antoniou A, Villalobos-Menuey E, Russo A, Trauger R, Vendemelio M et al. Characterization of a novel metabolic strategy used by drug-resistant tumor cells. *FASEB J* 2002; **16**: 1550–1557.

50. Mason KA, Withers HR, Davis CA. Dose dependent latency of fatal gastrointestinal and bone marrow syndromes. *Int J Radiat Biol* 1989; **55**: 1–5.

51. Terry NH, Travis EL. The influence of bone marrow depletion on intestinal radiation damage. *Int J Radiat Oncol Biol Phys* 1989; **17**: 569–573.

52. Nishimura EK, Granter SR, Fisher DE. Mechanisms of hair graying: incomplete melanocyte stem cell maintenance in the niche. *Science* 2005; **307**: 720–724.

53. Inomata K, Aoto T, Binh NT, Okamoto N, Tanimura S, Wakayama T et al. Genotoxic stress abrogates renewal of melanocyte stem cells by triggering their differentiation. *Cell* 2009; **137**: 1088–1099.

54. Aoki H, Hara A, Motohashi T, Kunisada T. Protective effect of Kit signaling for melanocyte stem cells against radiation-induced genotoxic stress. *J Invest Dermatol* 2011; **131**: 1906–1915.

55. Masuda Y, Kamiya K. Molecular nature of radiation injury and DNA repair disorders associated with radiosensitivity. *Int J Hematol* 2012; **95**: 239–245.

56. Thotala D, Chetyrkin S, Hudson B, Hallahan D, Voziyan P, Yazlovitskaya E. Pyridoxamine protects intestinal epithelium from ionizing radiation-induced apoptosis. *Free Radic Biol Med* 2009; **47**: 779–785.

57. Thotala DK, Geng L, Dickey AK, Hallahan DE, Yazlovitskaya EM. A new class of molecular targeted radioprotectors: GSK-3beta inhibitors. *Int J Radiat Oncol Biol Phys* 2010; **76**: 557–565.

58. Potten CS. Extreme sensitivity of some intestinal crypt cells to X and gamma irradiation. *Nature* 1977; **269**: 518–521.

Supplementary Information accompanies this paper on Cell Death and Disease website (http://www.nature.com/cddis)